

Performance of an X-ray single pixel TES microcalorimeter under DC and AC biasing

L.Gottardi*, J.van der Kuur*, P.A.J. de Korte*, R. Den Hartog*, B. Dirks*, M. Popescu*, H.F.C.Hoevers*, M.Bruijn*, M.Parra Borderias[†] and Y.Takei**

*SRON Netherlands Institute for Space Research, Sorbonnelaan 2, 3584CA, Utrecht, The Netherlands

[†]Instituto de Ciencia de Materiales de Aragon CSIC - Universidad de Zaragoza Facultad de Ciencias 50009 Zaragoza SPAIN

**ISAS-Jaxa, Japan

Abstract. We are developing Frequency Domain Multiplexing (FDM) for the read-out of TES imaging microcalorimeter arrays for future X-ray missions like IXO. In the FDM configuration the TES is AC voltage biased at a well defined frequencies (between 0.3 to 10MHz) and acts as an AM modulating element. In this paper we will present a full comparison of the performance of a TES microcalorimeter under DC bias and AC bias at a frequency of 370kHz. In both cases we measured the current-to-voltage characteristics, the complex impedance, the noise, the X-ray responsivity, and energy resolution. The behaviour is very similar in both cases, but deviations in performances are observed for detector working points low in the superconducting transition ($R/R_N < 0.5$). The measured energy resolution at 5.89keV is 2.7eV for DC bias and 3.7eV for AC bias, while the baseline resolution is 2.8eV and 3.3eV, respectively.

Keywords: FDM, multiplexing, TES microcalorimeter, X-ray detectors, IXO

PACS: 07.20.Fw,07.85.Nc,85.25.Am,85.25.Oj,95.55.-n

INTRODUCTION

We are developing an imaging array of Transition Edge Sensor (TES) microcalorimeters and bolometers for future X-ray and Infrared astronomy mission like IXO (International X-ray Observatory) and SPICA. The experiment described here is part of the European-Japanese project EURECA, which aims to demonstrate technological readiness of a 5 x 5 pixel array of TES-based microcalorimeters read-out by two SQUID-amplifier channels using frequency-domain-multiplexing (FDM) [5]. FDM requires amplitude modulation (AM) of the TES signal and it can be achieved by biasing the TES with an AC voltage bias source in a LC resonant circuit. It is essential to demonstrate that the observed good performance of a single pixels under constant voltage bias are maintained even when the TES works as a modulator. Several AC bias experiments with TESa have been performed so far with micro-calorimeter [1] and bolometers [2]. In this paper we will present a full comparison of the performance of a high resolution X-ray TES microcalorimeter under DC bias and AC bias at a frequency of 370kHz.

EXPERIMENTAL DETAILS

The detector has been integrated in a Janis two-stage ADR cooler precooled at 3.5 K by a mechanical Cryomech Pulse Tube (PT). A description of the measure-

ment set-up can be found in [4]. The sensor is a single-pixel of a 5x5 array and consists of a central Cu absorber on top of a Ti/Au TES deposited on a Si_xN_y membrane, which provides a weak thermal link to the ADR bath temperature. The transition temperature of the TES is $T_C \sim 100mK$, and the normal state resistance is $R_N = 143m\Omega$. All the measurements presented here have been taken at a bath temperature of $T=73mK$ and zero magnetic field perpendicular to the TES. A full characterization of this pixel under DC bias has been previously described in[3, 4].

The current through the TES was measured by a 100-SQUID array [8] operated in flux locked loop (FLL). The inductance of the SQUID input coil is $L_s \sim 70$ nH. The SQUID array is direct read out by a low noise commercial PTB-Magnicon electronics [9] in the DC bias case and by a FrontEndElectronics(FEE) developed at SRON in the AC bias case.

The scheme of the AC bias circuit is shown in Fig. 1.

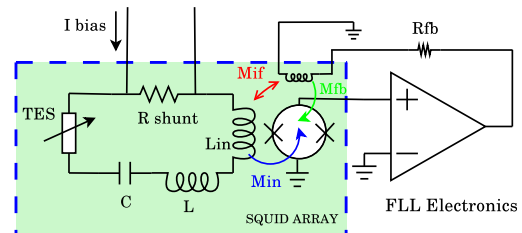


FIGURE 1. Schematic drawing of AC bias and read-out circuit.

The TES is voltage biased with an alternating bias current (AC) through a shunt resistance. The resistance change of the TES, induced by the detection of a photon, amplitude modulates the AC current flowing through the TES. Under AC voltage bias $V(t)$, the Joule power term ($V^2 \sin^2(\omega_0 t)/R_o$) switches on and off periodically with twice the biasing frequency $f_0 = \omega_0/2\pi$. The capacitor C and the total $L_{tot} = L_{in} + L$ define the bias circuit resonant frequency $f_0 = 1/(2\pi\sqrt{L_{tot}C})$. In the experiment described here we use discrete components for L and C: L is a 700nH coil made of a Nb wire wound around a Teflon cylinder and C is an NP0 capacitor with nominal value $C=220$ nF. The SQUID read-out amplifier is operated in a classical flux locked loop (FLL).

RESULTS

Current-voltage characteristic

The Fig 2 shows the current-to-voltage (I-V) and the power-to-voltage (P-V) characteristics of the microcalorimeter for both DC and AC bias.

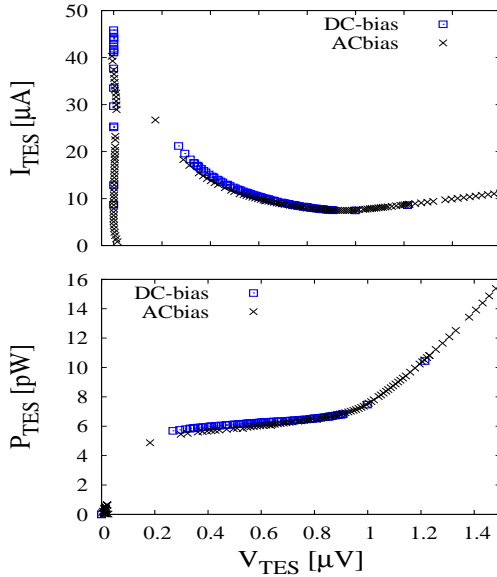


FIGURE 2. Current and power to voltage characteristics under DC and AC bias.

The curves overlaps for high TES bias voltage. Low in the transition a small deviation between the curves is observed. This effect may be due to the non-linear behaviour of the TES resistance when the detector is AC biased, since the resistance is a function of the sinusoidal bias current [1]. This effect is difficult to quantify and model because it depends on the dynamics of the superconductor in the transition and it is very likely geometry dependent. It may also be the result of a switching mech-

anism between two or more current paths in the detector occurring at every cycle of the carrier signal. Fig 3 shows the normalised resistance versus the normalised temperature curve derived from the I-V characteristics. The transition is clearly broadened in the AC bias case. For the same bias temperature lower in the transition the effective TES resistance under AC bias is about a factor of 2 higher.

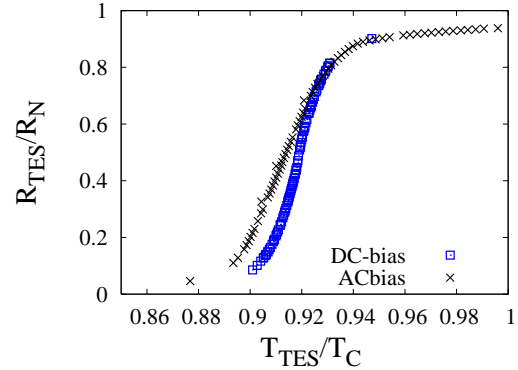


FIGURE 3. Normalised resistance R/R_N versus normalised temperature T/T_C for the DC and AC bias TES.

Impedance measurements

From the measurements of the TES impedance $Z_{TES}(\omega)$ we can derive the parameters, which characterise the thermal and electrical response of the TES [6]. The experimental data can be fitted using a second order system involving the TES plus absorber heat capacity and a dangling heat capacitance connected to the TES-Absorber system via a thermal conductance G_A , as described in [3]. The parameters $\alpha = \partial \ln R / \partial \ln T$, $\beta = \partial \ln R / \partial \ln I$, the total heat capacity $C = C_{TES} + C_{ABS}$ and the detector effective time constant are plotted in Fig 4 as a function of the normalised TES resistance.

The major difference between the AC and DC bias case is observed in the α and β parameters describing the sensitivity of the TES resistance on the temperature (α) and on the current (β) respectively. Under DC bias both the parameters are larger, specially lower in the transition, and show a peak at about $R/R_N = 0.5$. Features like this are often observed in our pixels: they are reproducible, but magnetic field and pixel dependent. They may be caused by the inhomogeneous current distribution in the TES. Under AC bias this effect could be smoothed out by the change of the current direction during a carrier cycle.

The value of α and β derived from $Z_{TES}(\omega)$ is consistent with the value $\alpha_N = \alpha / (1 + \beta/2)$ derived from the R-T characteristic obtained from the IV curve (Fig. 3).

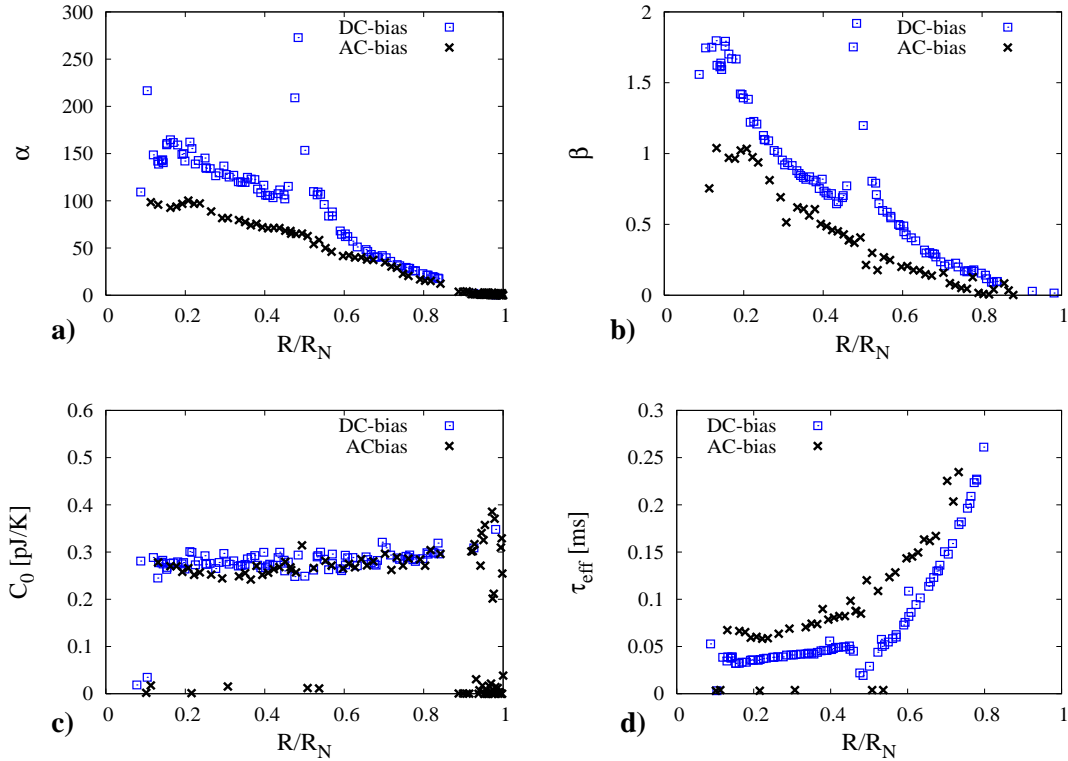


FIGURE 4. The parameters α, β , the total heat capacity $C = C_{TES} + C_{ABS}$ and the detector effective time constant are plotted, in **a, b, c** and **d**, as a function of the bias point for both the DC and AC bias case.

Noise analysis

One can use the parameters obtained from the complex impedance to model the detector noise. In Fig 5 the noise spectra at the operating point $R/R_N = 0.29$ is shown for the TES under DC bias (left) and AC bias (right). The results from the models are over-plotted. The model noise contributions are: phonon noise, TES Johnson noise thermal fluctuation noise (TFN) between TES-Absorber and dangling heat capacity. Those noise sources describe very well the noise observed at frequency below 5kHz both in the DC and AC bias configuration. In the frequency range where the Johnson noise is mainly dominant a non-modelled noise is present in the device. A useful parameterisation of the unexplained noise is done by defining it in terms of M -times the Johnson noise, like in Ullom et al.[7]. Both the DC and AC bias we observe $M < 1$ at $R/R_N > 0.5$ and $M > 1$ at bias point lower in the transition.

X-ray energy resolution

We measured the energy resolution of the microcalorimeter by acquiring the energy histogram of

the $K\alpha$ complex at 5.89keV of a Fe^{55} X-ray source. Due to the relatively small heat capacity of the pixel under study the device does not operate in the small signal regime when a 6keV photon is absorbed. The best energy resolution is generally observed when the microcalorimeter is at $R/R_N \sim 0.2$. Low in the transition the detector is faster and has an effective time constant of about $100\mu\text{s}$.

Under DC an X-ray energy resolution of $2.8 \pm 0.2\text{eV}$ and a baseline resolution of $2.7 \pm 0.2\text{eV}$ at the optimum working point $R/R_N = 0.17$. Under AC bias the best observed X-ray energy resolution is of $3.7 \pm 0.3\text{eV}$. Nominal value of the X-ray energy resolution measured under AC bias are however worse and fluctuates between 5eV and 6eV. The baseline resolution is generally always better than the X-ray resolution and is equal to $3.3 \pm 0.2\text{eV}$. Due to the large inductance used in the circuit the lowest point in the transition, achievable before oscillation in the electro-thermal feedback occur, is $R/R_N = 0.3$. This results in a detector which is slower and not optimally biased.

The performance of the TES pixel with a central absorber described in this paper is in general strongly dependent on the bias position. This is true both in the DC and AC bias conditions. Pixels with similar geometry

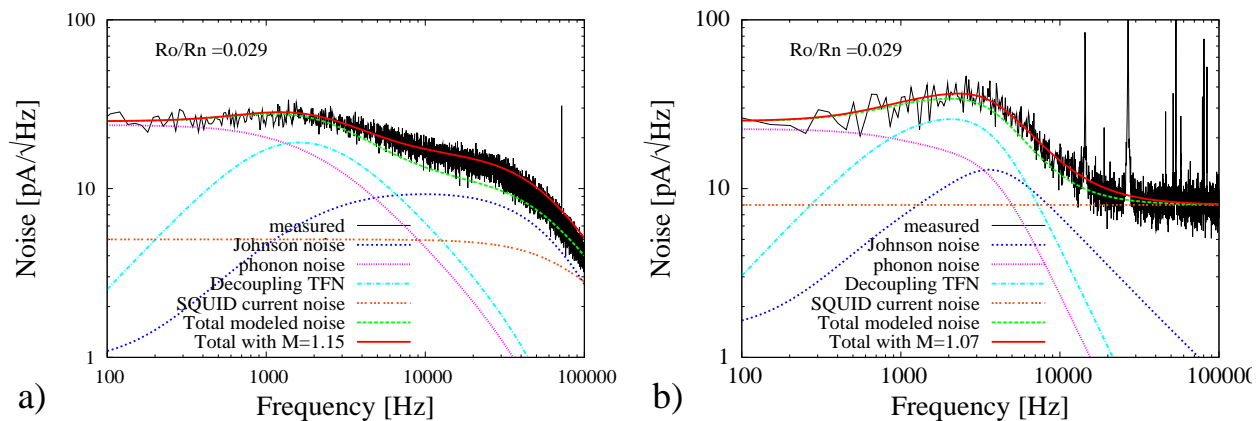


FIGURE 5. Noise spectra at $R/R_N = 0.29$ for a TES under DC bias (left) and AC bias (right). In both case the model explained well the observed noise. At this bias point a small excess noise is observed at high frequency with $M \neq 1$ in both cases.

have shown in the past bi-stable behaviour under DC bias and even stronger dependence of the energy resolution to the working point. We suspect that the broadening of the X-ray spectrum observed under AC bias may be caused by instability in the sensor itself: multiple current paths available in the TES, for example, could induce the sensor to change the bias point at any carrier cycle.

Other possible sources of instability external to the TES are: the carrier amplitude, the read out gain, the loop-gain in the SQUID FLL. We checked their stability in different configurations of FLL electronics, SQUIDS and carrier generators. Their contributions have been estimated to be smaller than 2eV.

CONCLUSION

We perform a full comparison of the performance of a single pixel TES microcalorimeter under DC and AC bias ($f_0 = 370\text{kHz}$), respectively. In both cases we measured the current-to-voltage characteristics, the complex impedance, the noise, the X-ray responsivity, and energy resolution.

The behaviour of the detector under AC bias begins to differ from the DC bias case at working point lower in the transition. We remark that the calibration of IV curves and complex impedance data taken under DC bias are very sensitive to offsets around zero current. A better analysis, including the error estimation on the parameters obtained from the I-V characteristics and complex impedance data is needed to guarantee a fair comparison.

Under DC an X-ray energy resolution of $2.8 \pm 0.2\text{eV}$ and a baseline resolution of $2.7 \pm 0.2\text{eV}$ at the optimum working point $R/R_N = 0.17$. Under AC bias the best observed X-ray energy resolution is of $3.7 \pm 0.3\text{eV}$. Nomi-

nal value of the X-ray energy resolution measured under AC bias are however worse and fluctuates between 5eV and 6eV. The baseline resolution is generally always better than the X-ray resolution and is equal to $3.3 \pm 0.2\text{eV}$.

In the future we are planning AC bias experiments using pixels with different geometry and at different resonant frequencies to better understand the behaviour of the detector as AM modulator.

ACKNOWLEDGMENTS

This work is financially supported by the Dutch Organisation for Scientific Research (NWO) and ESA's Technical Research Programme contract 5417. MPB would like to thank FPU program for predoctoral financial support.

REFERENCES

1. J. van der Kuur, et al, *Nucl. Instrum. Methods A.* **520**, 551-554, (2004)
2. A.T. Lee, et al, *Nucl. Instrum. Methods A.* **599**, 786-789, (2006)
3. Y. Takei, et al, *Journal of Low temperature Physics* **151**, (2008)
4. L. Gottardi, et al, *Journal of Low temperature Physics* **151**, (2008)
5. P.A. de Korte, et al, *Journal of Low temperature Physics* **151**, (2008)
6. M. Lindeman, et al, *Review of Scientific Instruments* **75**, 1283, (2004)
7. J.N. Ullom, et al, *Appl. Phys. Lett.* **87**, 194103, (2005)
8. Kindly provided by NIST
9. Magnicon-PTB, www.magnicon.com